



Preventing P-gp Ubiquitination Lowers A β Brain Levels in an Alzheimer's Disease Mouse Model

Anika M. S. Hartz^{1,2*}, Yu Zhong¹, Andrew N. Shen¹, Erin L. Abner¹ and Björn Bauer³

¹Sanders-Brown Center on Aging, University of Kentucky, Lexington, KY, United States, ²Department of Pharmacology and Nutritional Sciences, University of Kentucky, Lexington, KY, United States, ³Department of Pharmaceutical Sciences, College of Pharmacy, University of Kentucky, Lexington, KY, United States

OPEN ACCESS

Edited by:

Fahmeed Hyder,
Yale University, United States

Reviewed by:

Zemin Wang,
Harvard Medical School,
United States
Jessica Kate Hollen,
St-Vincent's Institute of Medical
Research, Australia
Ulrike Seifert,
Charité Universitätsmedizin Berlin,
Germany

*Correspondence:

Anika M. S. Hartz
anika.hartz@uky.edu

Received: 03 March 2018

Accepted: 05 June 2018

Published: 26 June 2018

Citation:

Hartz AMS, Zhong Y, Shen AN,
Abner EL and Bauer B
(2018) Preventing P-gp Ubiquitination
Lowers A β Brain Levels in an
Alzheimer's Disease Mouse Model.
Front. Aging Neurosci. 10:186.
doi: 10.3389/fnagi.2018.00186

One characteristic of Alzheimer's disease (AD) is excessive accumulation of amyloid- β (A β) in the brain. A β brain accumulation is, in part, due to a reduction in A β clearance from the brain across the blood-brain barrier. One key element that contributes to A β brain clearance is P-glycoprotein (P-gp) that transports A β from brain to blood. In AD, P-gp protein expression and transport activity levels are significantly reduced, which impairs A β brain clearance. The mechanism responsible for reduced P-gp expression and activity levels is poorly understood. We recently demonstrated that A β_{40} triggers P-gp degradation through the ubiquitin-proteasome pathway. Consistent with these data, we show here that ubiquitinated P-gp levels in brain capillaries isolated from brain samples of AD patients are increased compared to capillaries isolated from brain tissue of cognitive normal individuals. We extended this line of research to *in vivo* studies using transgenic human amyloid precursor protein (hAPP)-overexpressing mice (Tg2576) that were treated with PYR41, a cell-permeable, irreversible inhibitor of the ubiquitin-activating enzyme E1. Our data show that inhibiting P-gp ubiquitination protects the transporter from degradation, and immunoprecipitation experiments confirmed that PYR41 prevented P-gp ubiquitination. We further found that PYR41 treatment prevented reduction of P-gp protein expression and transport activity levels and substantially lowered A β brain levels in hAPP mice. Together, our findings provide *in vivo* proof that the ubiquitin-proteasome system mediates reduction of blood-brain barrier P-gp in AD and that inhibiting P-gp ubiquitination prevents P-gp degradation and lowers A β brain levels. Thus, targeting the ubiquitin-proteasome system may provide a novel therapeutic approach to protect blood-brain barrier P-gp from degradation in AD and other A β -based pathologies.

Keywords: blood-brain barrier, P-glycoprotein, Alzheimer's disease, brain capillaries, amyloid beta, ubiquitin-proteasome system, ubiquitin, proteasome

INTRODUCTION

Accumulation of amyloid- β (A β) in the brain is a neuropathological hallmark of Alzheimer's disease (AD; Hardy and Selkoe, 2002). Increasing evidence suggests that A β brain accumulation is due to impaired A β clearance from the brain (Zlokovic, 2005; Mawuenyega et al., 2010; Wang et al., 2016). Several studies indicate a role for the blood-brain barrier efflux transporter P-glycoprotein (P-gp)

in clearing A β from brain to blood: (1) P-gp transports A β *in vitro* (Lam et al., 2001; Kuhnke et al., 2007; Hartz et al., 2010); (2) in mice lacking P-gp, A β clearance is decreased while A β brain levels are increased (Cirrito et al., 2005; Yuede et al., 2016); (3) P-gp expression and transport activity are reduced at the blood-brain barrier of several AD mouse models (Hartz et al., 2010; Mehta et al., 2013; Park et al., 2014); and (4) treating human amyloid precursor protein (hAPP) mice with the PXR activator pregnenolone-16-carbonitrile (PCN) induces P-gp expression and activity, which restores A β transport and reduces A β brain levels (Hartz et al., 2010). (5) Results of multiple studies from different laboratories show that P-gp protein expression levels at the human blood-brain barrier are significantly reduced in AD patients (Wijesuriya et al., 2010; Jaynes and Provias, 2011; Carrano et al., 2014; Chiu et al., 2015). Consistent with reduced P-gp protein expression levels, results of recent PET imaging studies indicate compromised P-gp transport activity in AD patients compared to age-matched cognitive healthy individuals (van Assema et al., 2012; Deo et al., 2014). Thus, existing studies support the conclusion that blood-brain barrier P-gp is reduced in AD, however, more insights into the mechanism that triggers this phenomenon are needed to prevent P-gp loss in AD and improve A β brain clearance.

In this regard, we recently reported that exposing isolated rat brain capillaries to A β ₄₀ at concentrations similar to those found in AD patients reduced P-gp protein expression and transport activity levels in a time- and concentration-dependent manner (Hartz et al., 2016). We showed that A β ₄₀ triggers ubiquitination, internalization, and proteasomal degradation of P-gp in isolated rat brain capillaries *ex vivo* (Akkaya et al., 2015; Hartz et al., 2016). Collectively, these results indicate that blood-brain barrier P-gp is part of an A β clearance system and that P-gp expression and transport activity levels are reduced in AD, suggesting a link between high A β levels and reduced brain capillary P-gp levels in AD pathology.

In the present study, we show that P-gp protein expression and transport activity levels are reduced and that P-gp protein is highly ubiquitinated in isolated human brain capillaries from AD patients compared to P-gp in brain capillaries isolated from age-matched cognitive normal individuals. We extended our previous *ex vivo* findings to *in vivo* studies with hAPP mice by blocking P-gp ubiquitination in hAPP mice, which is the initial step of protein degradation mediated by the ubiquitin-proteasome system. We used transgenic hAPP-overexpressing mice (Tg2576) to test the hypothesis that preventing P-gp reduction results in a reduction of A β brain levels. We show here that inhibiting P-gp ubiquitination *in vivo* with PYR41, a cell-permeable, irreversible inhibitor of the ubiquitin-activating enzyme E1, prevents P-gp reduction at the blood-brain barrier and significantly lowers A β brain levels *in vivo*.

Together, our findings suggest that targeting the ubiquitin-proteasome system by inhibiting ubiquitination protects brain capillary P-gp and thereby lowers A β brain levels.

MATERIALS AND METHODS

Experimental Design and Statistical Analysis

Sample size (animal numbers, number of brain capillaries, number of human tissue samples) for individual experiments were based on power analyses of preliminary data and previously published data (Hartz et al., 2010, 2016, 2017), and are given in the corresponding figure legends. Number of repetitions are stated in the results section and the figure legends.

Results are presented as mean \pm SEM. One-way analysis of variance (ANOVA) was used to assess differences in group means. Pre-planned pairwise *post hoc* tests were carried out when the overall F test was significant, and the Bonferroni correction was used to control the type 1 error rate. Statistical significance was set at $\alpha = 0.05$. Data were analyzed using GraphPad Prism[®] statistical software (version 7.00; RRID:SCR_002798).

Animals

All animal experiments were approved by the University of Kentucky Institutional Animal Care and Use Committee (Protocol #2014-1233; PI: AMS Hartz) and carried out in accordance with AAALAC regulations, the US Department of Agriculture Animal Welfare Act, and the Guide for the Care and Use of Laboratory Animals of the NIH.

Male transgenic hAPP-overexpressing mice (Tg2576 strain; 129S6.Cg-Tg(APP_{SWE})2576Kha; RRID:IMSR_TAC:2789; $n = 45$) and corresponding male wild type (WT) mice ($n = 15$; RRID:IMSR_TAC:2789) were purchased from Taconic Farms (Germantown, NY, USA). On arrival, mice were 8-week old with an average body weight of 27.1 ± 2.6 g (SD) for WT mice and 29.9 ± 2.9 g (SD) for hAPP mice. Animals were single-housed in an AALAC-accredited temperature- and humidity-controlled vivarium (23°C, 60%–65% relative humidity, 14:10 light-dark cycle) in cages connected to an EcoFlo Allentown ventilation system (Allentown Inc., Allentown, NJ, USA). Animals had *ad libitum* access to tap water and standard rodent feed (Harlan Teklad Chow 2918, Harlan Laboratories Inc., Indianapolis, IN, USA) and were allowed to habituate to the vivarium for at least 2 weeks after arrival before the start of experiments.

Human Brain Tissue Samples

Human brain tissue samples (inferior parietal lobule) were obtained from the UK-ADC tissue bank (IRB #B15-2602-M). Case inclusion criteria for this study were enrollment in the UK-ADC longitudinal autopsy cohort (Nelson et al., 2007), a post-mortem interval ≤ 4 h, and a final consensus diagnosis determined by a group of UK-ADC neuropathologists, neuropsychologists, and neurologists. Cases were classified into two groups: Group (1) cognitive normal ($n = 3$; a classification of “normal” denotes a consensus diagnosis of normal cognition and CERAD rating of “criteria not met”) and Group (2) AD patients ($n = 3$; Mirra et al., 1991). All brain tissue samples were from female individuals, whose average age at death was 85.5 ± 9.2 years (group 1, cognitive normal, post-mortem interval: 1.5 h \pm 0.3 h, Braak stage score: 1 ± 0).

and 86.5 ± 9.2 years (group 2, AD, post-mortem interval: $3.5 \text{ h} \pm 0.7 \text{ h}$, Braak stage score: 5.5 ± 0.7).

Chemicals

Antibodies against β -actin (ab8226; RRID:AB_306371), human A β 40 (ab12265; RRID:AB_298985), human A β 42 (ab12267; RRID:AB_298987), LRP (ab92544; RRID:AB_2234877), RAGE (ab3611; RRID:AB_303947), APP (ab11118; RRID:AB_442855) and 20S proteasome (ab109530; RRID:AB_10860339; antibody raised against a synthetic peptide within the human proteasome 20S C2 unit (amino acids: 250–350; C terminal)), as well as cyclosporine A (CSA; ab120114) were purchased from Abcam (Cambridge, MA, USA). Modified Dulbecco's phosphate buffered saline (DPBS; with 0.9 mM Ca^{2+} and 0.5 mM Mg^{2+}) was purchased from HyClone (Logan, UT, USA). CompleteTM protease inhibitor was purchased from Roche (Mannheim, Germany). C219 antibody against P-gp was purchased from ThermoFisher (MA126528; RRID:AB_795165; Waltham, MA, USA). Fluorescein-hA β ₄₂ [fluorescein-A β _(1–42)] was purchased from rPeptide (Bogart, GA, USA). [N-(4-nitrobenzofurazan-7-yl)-D-Lys8]-cyclosporine A (NBD-CSA) was custom-synthesized by R. Wenger (Basel, Switzerland; Wenger, 1986). PSC833 was a kind gift from Novartis (Basel, Switzerland). PYR41, CelLyticTM M, Ficoll[®] PM 400, bovine serum albumin and all other chemicals were purchased at the highest grade from Sigma-Aldrich (St. Louis, MO, USA).

PYR41 Dosing

Table 1 shows the dosing regimen for this *in vivo* study. Mice were dosed as follows: Group 1: WT mice ($n = 15$) received *i.p.* vehicle every third day and *p.o.* vehicle on both days between *i.p.* vehicle injections. Group 2: hAPP mice ($n = 15$) also received *i.p.* vehicle every third day and *p.o.* vehicle on both days between *i.p.* vehicle injections. Group 3: hAPP-PYR41 mice ($n = 15$) were dosed every third day with 2 mg/kg PYR41 by *i.p.* injection and received *p.o.* vehicle on days between PYR41 treatment. Group 4: hAPP-PYR41/CSA mice ($n = 15$) were dosed every third day with 2 mg/kg PYR41 by *i.p.* injection and received 25 mg/kg CSA via oral gavage on both days between doses of PYR41.

Blood Collection

Blood samples were collected by facial vein bleeding 24 h prior to the start of the first dose to obtain control values. Twenty-four hours after the last dose, mice were euthanized by CO₂ inhalation, decapitated and trunk blood was collected in heparinized blood collection tubes. Plasma was obtained by centrifugation at $5000 \times g$ for 15 min at 4°C and stored at –80°C until further analysis.

Brain Capillary Isolation

Brain capillaries were isolated using a modified method previously described elsewhere (Hartz et al., 2012). Briefly, mice were euthanized with CO₂ followed by decapitation. Brains were removed, cleaned, dissected and homogenized in DPBS containing $\text{Ca}^{2+}/\text{Mg}^{2+}$ and supplemented with 5 mM D-glucose

TABLE 1 | PYR41 dosing regimen.

Group	Day of treatment													
	1	2	3	4	5	6	7	8	9	10	11	12	13	14
WT	Vehicle (ip)	Vehicle (po)	Vehicle (po)	Vehicle (ip)	Vehicle (po)	Vehicle (po)	Vehicle (ip)	Vehicle (po)	Vehicle (po)	Vehicle (ip)	Vehicle (po)	Vehicle (po)	Vehicle (ip)	Vehicle (po)
hAPP	Vehicle (ip)	Vehicle (po)	Vehicle (po)	Vehicle (ip)	Vehicle (po)	Vehicle (po)	Vehicle (ip)	Vehicle (po)	Vehicle (po)	Vehicle (ip)	Vehicle (po)	Vehicle (po)	Vehicle (ip)	Vehicle (po)
hAPP-PYR41	PYR41 (ip)	Vehicle (po)	Vehicle (po)	PYR41 (ip)	Vehicle (po)	Vehicle (po)	PYR41 (ip)	Vehicle (po)	Vehicle (po)	PYR41 (ip)	Vehicle (po)	Vehicle (po)	PYR41 (ip)	Vehicle (po)
hAPP-PYR41/CSA	PYR41 (ip)	CSA (po)	CSA (po)	PYR41 (ip)	CSA (po)	CSA (po)	PYR41 (ip)	CSA (po)	CSA (po)	PYR41 (ip)	CSA (po)	CSA (po)	PYR41 (ip)	CSA (po)

The present dosing regimen was based on a 2-week preliminary dosing study with CD-1 mice (data not shown). WT and hAPP mice were treated according to the following dosing scheme over the course of 14 days: WT and hAPP mice were given vehicle *p.o.* by oral gavage or by *i.p.* injection once every 3 days. hAPP-PYR41 mice received 2 mg/kg PYR41 by *i.p.* injection once every 3 days and vehicle *p.o.* by oral gavage on all other days. hAPP-PYR41/CSA mice received 2 mg/kg PYR41 by *i.p.* injection once every 3 days and 25 mg/kg CSA *p.o.* by oral gavage on all other days.

and 1 mM sodium pyruvate. Ficoll® PM 400 was added to the homogenized brains (final concentration 15%) and the homogenate was centrifuged (5800 g, 20 min, 4°C). After centrifugation, the capillary-enriched pellet was collected and resuspended in 1% BSA-DPBS. The capillary suspension was first passed through a 300 µm nylon mesh and then passed over a glass bead column using 1% BSA-DPBS. Capillaries adhering to the glass beads were washed off and collected by agitation in 1% BSA-DPBS. After centrifugation (1500 g, 3 min, 4°C), the capillary pellet was washed three times with DPBS (no BSA), collected, and used for experiments or crude membrane isolation.

Brain Capillary Crude Membrane Isolation

Brain capillary crude membranes were isolated as previously described (Hartz et al., 2012). Freshly isolated brain capillaries were homogenized in lysis buffer (CelLytic™ M, Sigma-Aldrich, St. Louis, MO, USA) containing Complete™ protease inhibitor. Homogenates were centrifuged to separate the membrane fraction from organelles and debris (10,000 g, 15 min, 4°C), and the resulting membrane-containing supernatant was centrifuged to pellet capillary crude membranes (100,000 g, 90 min, 4°C). The resulting pellet containing brain capillary crude membranes was resuspended and stored at -80°C.

Aβ Immunostaining of Brain Capillaries

Aβ immunostaining of mouse brain capillaries was performed as previously described (Hartz et al., 2010). Briefly, isolated mouse brain capillaries were fixed with 3% paraformaldehyde/0.25% glutaraldehyde for 30 min at room temperature. After washing with PBS, capillaries were permeabilized with 0.5% Triton X-100 for 30 min and washed with PBS. Capillaries were blocked with 1% BSA/DPBS for 60 min and incubated overnight at 4°C with a 1:250 (4 µg/ml) dilution of rabbit polyclonal antibody to human Aβ1-40 (hAβ40; ab12265, Abcam, Cambridge, MA, USA; RRID:AB_298985) or rabbit polyclonal to human Aβ1-42 antibody (hAβ42; ab12267; Abcam, Cambridge, MA, USA; RRID:AB_298987). Capillaries were washed with 1% BSA/PBS and incubated with Alexa-Fluor 488-conjugated goat anti-rabbit IgG (1:1000, 1 µg/ml; Invitrogen, Carlsbad, CA, USA; RRID:AB_2576217) for 1 h at 37°C. Nuclei were counterstained with 1 µg/ml 4,6-diamidino-2-phenylindole (DAPI; MilliporeSigma, Burlington, MA, USA; RRID:SCR_014366). Aβ immunofluorescence was visualized with confocal microscopy (Leica TCS SP5 confocal microscope, 63× water objective, NA 1.2, Leica Instruments, Wetzlar, Germany).

From each treatment group, confocal images of seven capillaries were acquired. Aβ membrane immunofluorescence for each capillary was quantitated with ImageJ software v1.48 as previously described (Hartz et al., 2010). A 10 × 10 grid was superimposed on each image, and fluorescence measurements of capillary membranes were taken between intersecting grid lines. Fluorescence intensity for each capillary was the mean of three measurements per capillary.

Aβ ELISA

Human Aβ40 and Aβ42 levels were quantitated in plasma and brain samples by ELISA (KHB3482 (Sensitivity: <6 pg/ml) and KHB3442 (Sensitivity: <10 pg/ml) from Invitrogen, Camarillo, CA, USA) according to the manufacturer's protocol.

Plasma Samples

Blood samples were collected from control, PYR41 and PYR41/CSA-treated hAPP transgenic mice. Plasma was obtained from blood samples by centrifugation at 5000 g for 5 min at 4°C, and then diluted with standard diluent buffer provided with the ELISA kit. To determine hAβ40 levels, samples were diluted 1:50; to determine hAβ42 levels, samples were diluted 1:4.

Brain Samples

To determine brain hAβ40 and hAβ42 levels, brain tissue samples were homogenized in guanidine Tris-HCl buffer (5 M, pH 8) to extract Aβ. To determine hAβ40 levels, samples were diluted 1:20 in DPBS buffer containing 5% BSA and 0.03% Tween-20; to determine hAβ42 levels, samples were diluted 1:5. Diluted samples were centrifuged at 16,000 g for 20 min at 4°C; the supernatant was used for ELISA analysis.

Absorbance was measured at 450 nm using a Synergy™ H1 Hybrid Multi-Mode Reader (BioTek, Winooski, VT, USA). A standard curve was plotted using Gen5™ software v2.07 to determine the concentration of hAβ40 and hAβ42 in plasma and brain samples; values at 450 nm were corrected for background absorbance; four parameter logistic ELISA curve fitting was selected.

Western Blotting

Protein expression levels from various tissues were determined by Western blotting as described previously (Hartz et al., 2010, 2016). Protein concentration of brain capillary crude membranes was measured with the Bradford assay. Western blots were performed by using the Invitrogen NuPage® Bis-Tris electrophoresis and blotting system. After protein electrophoresis and transfer, blotting membranes were blocked and incubated overnight with the primary antibody as indicated. Membranes were washed and incubated for 1 h with horseradish peroxidase-conjugated ImmunoPure secondary IgG antibody (1:5000, 0.15 µg/ml; Thermo Fisher Scientific, Waltham, MA, USA). Proteins were detected with SuperSignal West Pico Chemoluminescent Substrate (Thermo Fisher Scientific, Waltham, MA, USA). Protein bands were visualized and recorded with a Bio-Rad ChemiDoc XRS+ gel documentation system (Bio-Rad Laboratories, Hercules, CA, USA). Image Lab 5.0 software from Bio-Rad Laboratories (RRID:SCR_014210) was used for densitometric analyses of band intensities and digital molecular weight analyses; the molecular weight marker was RPN800E (GE Healthcare, Chalfont St. Giles, Buckinghamshire, UK). Linear adjustments of contrast and brightness were applied to entire Western blot images. None of the Western blots shown were modified by nonlinear adjustments.

Immunoprecipitation

Immunoprecipitation was carried out as previously reported (Hartz et al., 2016). Briefly, brain capillaries were homogenized in lysis buffer (CelLytic™ M, Sigma-Aldrich, St. Louis, MO, USA) containing Complete™ protease inhibitor. Samples were centrifuged to separate cellular membranes from organelles and debris (10,000 g, 15 min, and 4°C). Protein concentration of the supernatants was determined by Bradford assay.

Anti-P-gp antibody (C219, EMD Millipore, Billerica, MA, USA) was coupled with Pierce Protein A/G Plus Agarose (Thermo Fisher Scientific, Waltham, MA, USA) beads overnight at 4°C in TBST (20 mM Tris (pH 8.0), 170 mM NaCl, 0.05% Tween 20) supplemented with 1% BSA. The immune complex was added to the cell lysate and incubated for 3 h at 4°C. Beads were washed with lysis buffer (10 mM Tris (pH 7.5), 2 mM EDTA, 100 mM NaCl, 1% NP-40, 50 mM NaF, 1 mM Na₃VO₄) containing Complete™ protease inhibitor. For ubiquitin immunoprecipitations, the Pierce™ Ubiquitin Enrichment Kit (#89899; Thermo Fisher Scientific, Waltham, MA, USA) was used according to the manufacturer's protocol. Immunoprecipitated proteins were eluted from agarose beads (IP: P-gp) or the ubiquitin affinity resin (IP: ubiquitin) with NuPAGE LDS sample buffer and heated at 70°C for 10 min. IP samples were resolved by SDS-PAGE and analyzed by Western blotting as described above.

Simple Western Assay

Human brain capillary membrane samples were mixed with Wes™ sample buffer and analyzed with a Simple Western assay designed for the Wes™ instrument by ProteinSimple as previously described (San Jose, CA, USA; Hartz et al., 2016). All steps of the Wes™ Master Kit assay were performed according to the manufacturer's protocol. Briefly, glass microcapillaries were loaded with stacking and separation matrices followed by sample loading. During capillary electrophoresis, proteins were separated by size and then immobilized to the capillary wall. P-gp and β -actin were identified with primary antibodies against P-gp (1:100, 3 μ g/ml, C219, MA126528, ThermoFisher, Waltham, MA, USA; RRID:AB_795165) and β -actin (1:150, 5 μ g/ml, ab8226, Abcam, Cambridge, MA, USA; RRID:AB_306371), respectively, followed by immunodetection using Wes™ Master Kit HRP conjugated anti-mouse secondary antibody and chemiluminescent substrate. Using Compass V. 2.6.5 software, electropherograms were generated for each sample and each protein (P-gp and β -actin). The area under the curve (AUC), which represents the signal intensity of the chemiluminescent reaction was analyzed for P-gp and β -actin. Values given for P-gp protein expression were normalized to β -actin.

P-gp Transport Assay

To determine P-gp transport activity, freshly isolated brain capillaries from WT and hAPP mice were incubated for 1 h at room temperature with the fluorescent P-gp-specific substrate NBD-CSA (2 μ M in PBS buffer; Hartz et al., 2004, 2008, 2010). To assess P-gp-mediated A β transport, isolated brain capillaries were incubated for 1 h at room temperature with 5 μ M fluorescein-hA β 42 in DPBS buffer (Hartz et al., 2010). For each

treatment, images of 10 capillaries were acquired by confocal microscopy using the 488 nm line of an argon laser (Leica Instruments, Wetzlar, Germany) of a Leica TCS SP5 confocal microscope with a 63 \times 1.2 NA water immersion objective. Images were analyzed by quantitating NBD-CSA fluorescence in the capillary lumen using Image J v.1.48v (Wayne Rasband, NIH, USA; RRID:SCR_003070). Specific, luminal NBD-CSA fluorescence was taken as the difference between total luminal fluorescence and fluorescence in the presence of the P-gp-specific inhibitor PSC833 (5 μ M; Hartz et al., 2004, 2008, 2010).

RESULTS

P-gp Ubiquitination Levels Are Increased in Brain Capillaries From AD Patients

Several studies have provided evidence showing that P-gp expression levels at the blood-brain barrier are reduced in AD patients compared to control individuals (Wijesuriya et al., 2010; Jaynes and Provias, 2011; Carrano et al., 2014; Chiu et al., 2015). To assess P-gp protein expression in human brain capillaries, we utilized a recently established protocol to isolate brain capillaries from fresh human frontal cortex tissue (Hartz et al., 2017). **Figure 1** shows representative confocal images of a brain capillary isolated from brain tissue of a cognitive-normal individual (CNI) immunostained for P-gp (**Figure 1A**). The negative control (no primary antibody) shows no signal for P-gp (**Figures 1B,B1**: green channel; **B2**: blue channel; **B3**: overlay of green and blue channel; **B4**: transmitted light channel).

We utilized the Simple Western™ assay to quantitate P-gp protein levels in isolated human brain capillaries. This novel assay allows protein quantitation at 10-fold higher sensitivity and better reproducibility compared to Western blotting (Hartz et al., 2017). The assay is based on automated microcapillary electrophoresis; data robustness was tested at the NIH (Chen et al., 2015). **Figure 1C** shows that a band for P-gp was detected in membrane samples of brain capillaries isolated from CNI patients that was between the 180 kDa and 230 kDa bands of the molecular weight marker. Consistent with previous studies (Wijesuriya et al., 2010; Jaynes and Provias, 2011; Carrano et al., 2014; Chiu et al., 2015), we found that P-gp protein levels in brain capillary samples from AD patients were significantly lower compared to brain capillaries from cognitive normal individuals (CNI; **Figure 1C**); β -actin served as loading control. **Figure 1D** shows the electropherogram of the P-gp microcapillary electrophoresis. Analysis of this electropherogram revealed that the P-gp band peaked at 199.8 ± 2.5 kDa; the peak for β -actin was detected at 49.7 ± 2.6 kDa. The bandwidth for P-gp was 24.8 ± 1.9 kDa and ranged from 187.4 kDa to 212.2 kDa; the bandwidth for β -actin was 9.3 ± 1.2 kDa and ranged from 45.1 kDa to 54.35 kDa. In these electropherograms, each AUC is proportional to the amount of protein, allowing comparisons of P-gp levels between CNI and AD patients. Utilizing this method, we found that P-gp protein levels in capillaries isolated from brain tissue of AD patients are 37%

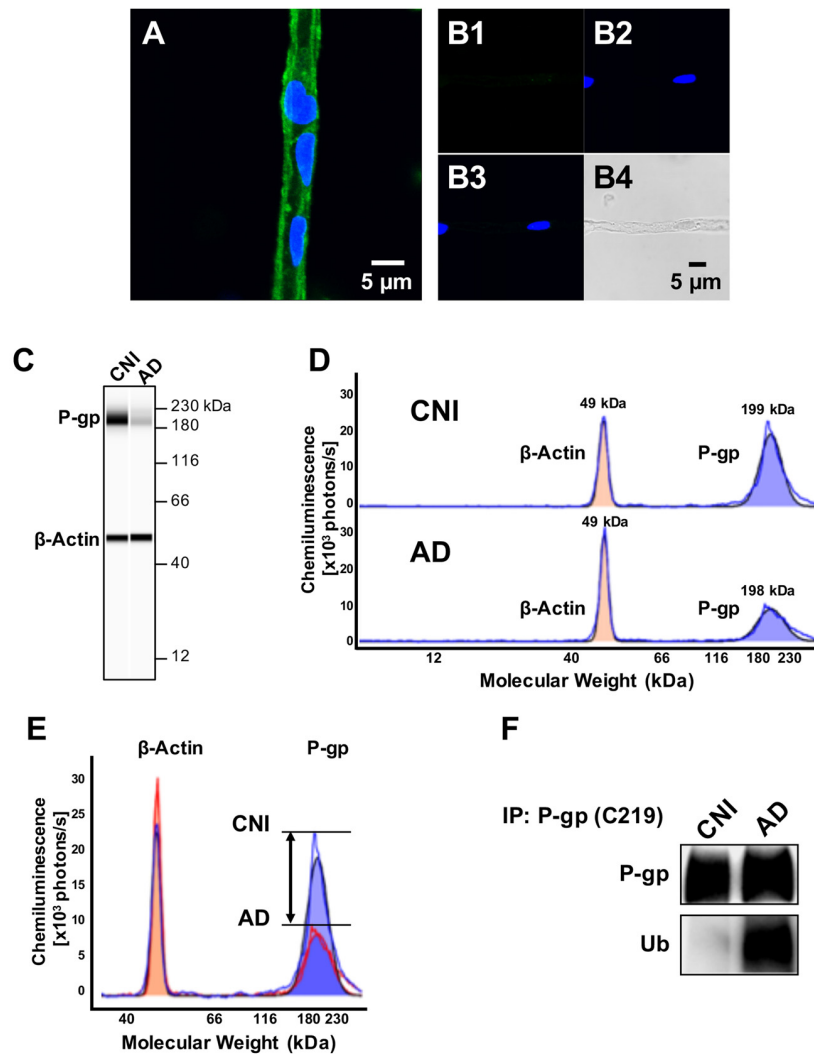


FIGURE 1 | P-glycoprotein (P-gp) protein expression levels are decreased and P-gp ubiquitination levels are increased in brain capillaries from Alzheimer's disease (AD) patients. **(A)** Representative image of a P-gp-immunostained (green) brain capillary isolated from brain tissue of a cognitive normal individual (CNI); nuclei were counterstained with DAPI (blue). **(B)** Negative control (no primary antibody): **(B1)**; green channel; **(B2)**; blue channel; **(B3)**; overlay of green and blue channel) and **(B4)**; transmitted light channel). **(C)** Representative WES™ image and **(D)** electropherogram showing reduced P-gp (blue shaded area) protein expression levels in brain capillaries isolated from human brain tissue (frontal cortex) of AD patients ($n = 3$) vs. CNIs ($n = 3$). **(E)** Overlay of electropherograms displayed in **(D)** show a reduction in the area under the curve (AUC) that represents P-gp protein expression levels (blue shaded area) in brain capillaries from AD patients (red line) relative to CNI (blue line). In contrast, β -actin levels (orange shaded area) in brain capillaries from AD patients (red line) and CNI (blue line) were the same. **(F)** Western blot showing that ubiquitin levels in P-gp-immunoprecipitates are increased in capillaries from AD patients compared to those from CNI.

lower compared to P-gp protein levels in capillaries isolated from brain samples of CNI (AUC P-gp AD 349670 vs. AUC Pgp CNI 557147 photons \times kDa/s). **Figure 1E** shows an overlay of the electropherograms in **Figure 1D**. This overlay shows the difference in peak heights and the areas under the curve (AUC) that represent total protein amount for P-gp and β -actin, respectively, which is a more accurate approach to quantitate protein amount than optical density measurements (O'Neill et al., 2006).

To determine ubiquitinated P-gp levels, we performed immunoprecipitation experiments with brain capillaries from brain tissue of CNI and AD patients and observed that

ubiquitination of P-gp was 2.8-fold higher in brain capillaries from patients with AD compared to CNI ($n = 3$; $p = 0.05$, **Figure 1F**; Supplementary Figures S1A,B). This indicates that blood-brain barrier P-gp is highly ubiquitinated in patients with AD.

PYR41 Prevents Reduction of P-gp Expression and Activity Levels in hAPP Mice

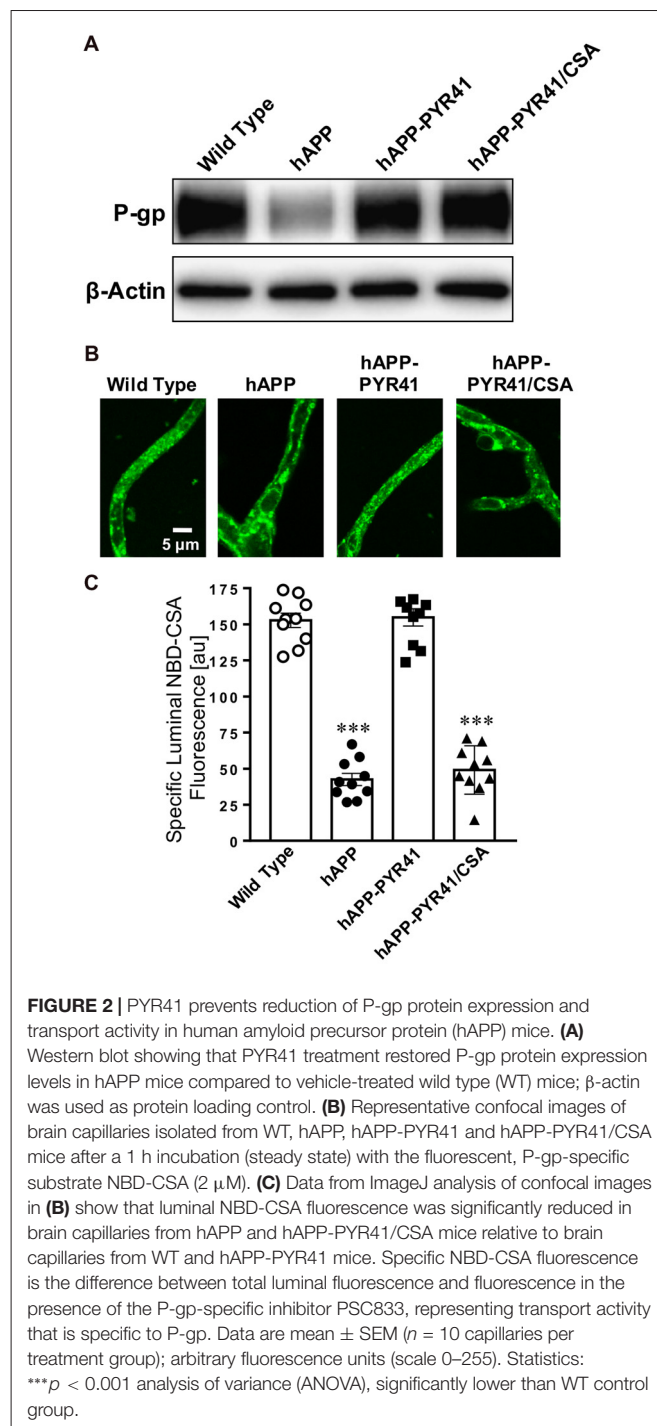
Ubiquitination of a target protein is carried out by three enzymes. First, ubiquitin is activated by the ubiquitin-activating enzyme

E1. In the second step, ubiquitin is transferred onto the target protein by the conjugating enzyme E2. This ubiquitin transfer is completed in a third step by the ubiquitin ligase E3 resulting in ubiquitination of the target protein.

PYR41 is an E1 ubiquitin-activating enzyme-specific inhibitor that shows little activity on E2 and E3. PYR41 irreversibly blocks ubiquitination, thereby preventing ubiquitin-mediated proteasomal degradation *in vitro* and *in vivo* (Yang et al., 2007; Guan and Ricciardi, 2012). We used PYR41 to test the hypothesis that blocking ubiquitination protects blood-brain barrier P-gp from degradation in transgenic hAPP mice *in vivo*. We dosed young, 8-week old hAPP mice with 2 mg/kg PYR41 i.p. once every 3 days for 14 days (Table 1). An additional group of mice received PYR41 in combination with the P-gp inhibitor cyclosporin A (CSA; 25 mg/kg, p.o.) on days between dosing PYR41 alone. These PYR41/CSA-treated mice serve as control group for P-gp transport activity and are used to account for PYR41-treatment effects that depend on P-gp transport activity. WT and hAPP control mice received vehicle. Treatment of hAPP mice with PYR41 restored P-gp protein expression levels in brain capillary membranes to levels observed in vehicle-treated WT mice (Figure 2A). We also observed this effect in PYR41/CSA-treated animals. Optical density measurements of P-gp ($n = 3$, normalized to β -actin) given as percent of WT control mice (SEM, p -value) are: hAPP: $46 \pm 10.5\%$ ($t = 3.52$, $p = 0.022$; ANOVA *post hoc* test); hAPP-PYR41: $106 \pm 11.8\%$ ($t = 0.39$, $p = 0.72$; ANOVA *post hoc* test), and hAPP-PYR41/CSA: $106 \pm 10.4\%$ ($t = 0.39$, $p = 0.70$; ANOVA *post hoc* test).

Next, we determined P-gp transport activity in isolated brain capillaries by using a transport assay we previously described (Hartz et al., 2008, 2010, 2016, 2017). In this assay, freshly isolated brain capillaries are incubated with the fluorescent P-gp substrate NBD-cyclosporin A (NBD-CSA, 2 μ M) for 1 h to steady state. Capillaries are then imaged with a confocal microscope followed by quantitative image analysis of NBD-CSA fluorescence in the capillary lumen. In brain capillaries with lower P-gp transport activity compared to control capillaries, less NBD-CSA is transported into the capillary lumen, resulting in lower luminal NBD-CSA fluorescence. Thus, the level of luminal NBD-CSA fluorescence is a measure for P-gp transport activity.

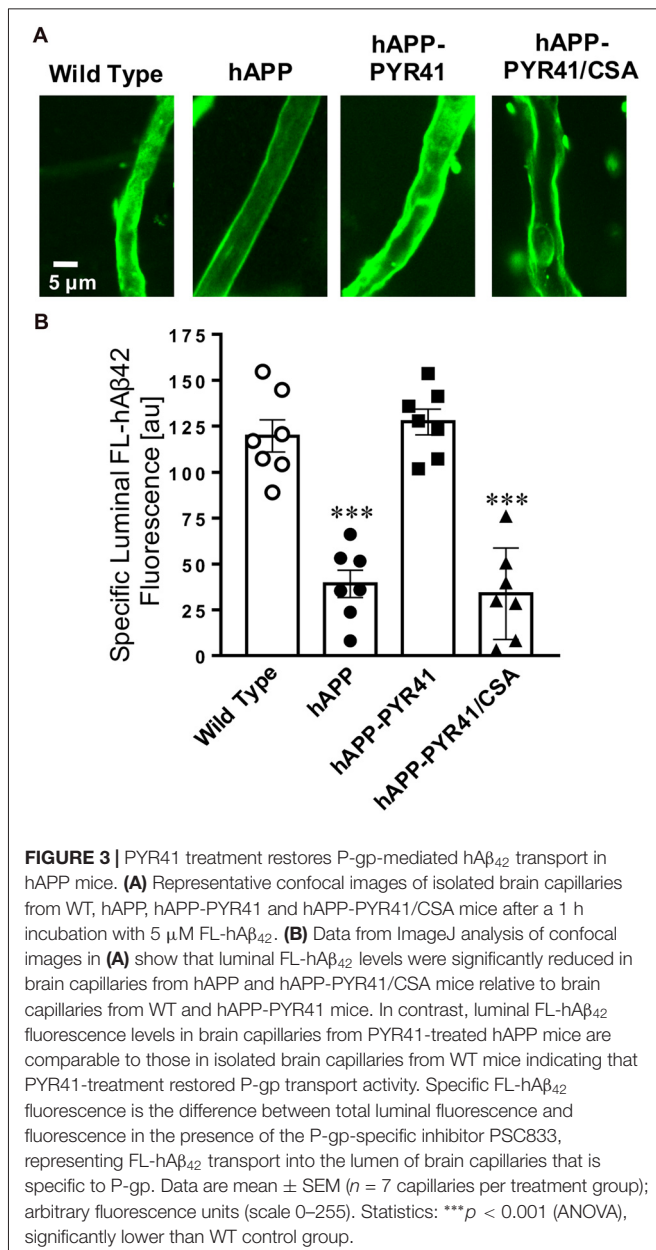
Figure 2B shows representative confocal images of brain capillaries isolated from WT mice, hAPP mice, hAPP mice treated with PYR41 and hAPP mice treated with PYR41/CSA that were exposed to NBD-CSA. Compared to capillaries from WT mice, luminal NBD-CSA fluorescence was decreased in capillaries from hAPP mice and PYR41/CSA-treated hAPP mice, indicating reduced P-gp transport activity levels. In contrast, PYR41 treatment maintained luminal NBD-CSA fluorescence in capillaries from hAPP mice at control levels. Data from confocal image analysis indicate that specific luminal NBD-CSA fluorescence in the lumens of brain capillaries from hAPP mice was reduced by 72% ($t = 15.1$, $p < 0.0001$; ANOVA *post hoc* test) relative to WT mice (Figure 2C). In contrast, luminal NBD-CSA fluorescence levels in brain capillaries from PYR41-treated hAPP mice were similar to levels measured in capillaries



from WT mice ($t = 0.3$, $p = 0.81$; ANOVA *post hoc* test). In brain capillaries from PYR41-treated hAPP mice that also received CSA to control for P-gp transport activity luminal NBD-CSA fluorescence was reduced by 68% relative to WT mice; this reduction is comparable to that seen in vehicle-treated hAPP mice ($t = 13.0$, $p < 0.0001$; ANOVA *post hoc* test).

We repeated this experiment using fluorescein-hA β_{42} (FL-hA β_{42}) to test the ability of P-gp to transport hA β into the

lumen of brain capillaries. **Figure 3A** shows representative images of isolated brain capillaries incubated to steady state for 1 h with 5 μ M FL-hA β ₄₂. Image analysis shows that luminal FL-hA β ₄₂ fluorescence was reduced to $32.6 \pm 9.2\%$ ($t = 6.4$, $p < 0.0001$; ANOVA *post hoc* test) in capillaries from hAPP mice relative to capillaries from WT mice (**Figure 3B**). Luminal FL-hA β ₄₂ fluorescence levels in brain capillaries isolated from PYR41-treated hAPP mice was comparable to fluorescence levels observed in capillaries from WT mice ($t = 0.6$, $p = 0.54$; ANOVA *post hoc* test). In contrast, FL-hA β ₄₂ fluorescence levels in capillary lumens from PYR41/CSA-treated control mice were significantly reduced ($t = 6.87$, $p < 0.0001$; ANOVA *post hoc* test), which was comparable to luminal fluorescence levels in brain capillary lumens of untreated hAPP mice.



Together, the data in **Figures 2, 3** demonstrate that PYR41 treatment of young hAPP mice attenuated reduction of both P-gp protein expression and transport activity levels. This suggests that PYR41 prevented P-gp degradation through the ubiquitin-proteasome system.

PYR41 Treatment of hAPP Mice Prevents P-gp Ubiquitination *in Vivo*

PYR41 is a cell-permeable, specific and irreversible inhibitor of the ubiquitin-activating enzyme E1, which is responsible for mediating the first step of ubiquitination of proteins that are proteasome targets. Thus, PYR41 inhibits ubiquitination of proteins, thereby preventing their degradation by the ubiquitin-proteasome system. To determine the effect of PYR41 treatment on the ubiquitination status of P-gp at the blood-brain barrier, we performed immunoprecipitation experiments with isolated brain capillaries from PYR41-treated and untreated hAPP mice. The Western blot in **Figure 4A** shows that immunoprecipitated P-gp protein levels were similar in brain capillaries from hAPP mice and hAPP mice treated with PYR41 and PYR41/CSA. We observed high levels of ubiquitinated P-gp in isolated capillaries from hAPP mice. In contrast, brain capillaries isolated from PYR41 and PYR41/CSA-treated hAPP mice had no detectable levels of ubiquitinated P-gp. These data indicate that PYR41 treatment was effective to prevent ubiquitination of P-gp in brain capillaries.

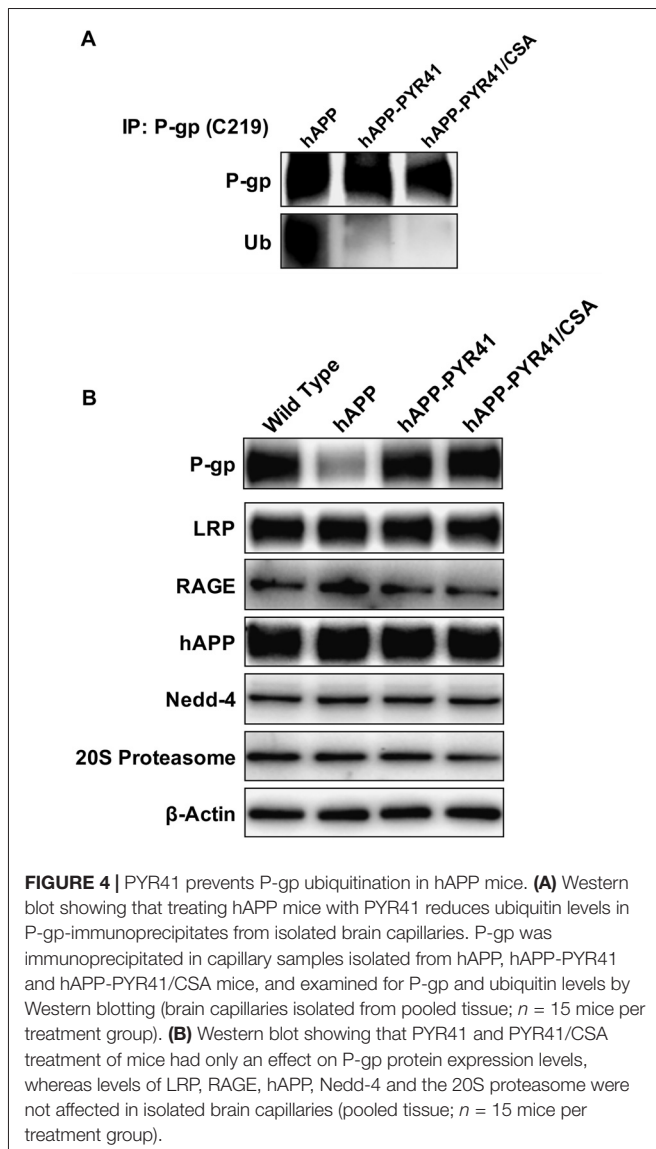
The Western blot in **Figure 4B** shows protein expression levels of P-gp and other proteins involved in A β production or transport, as well as signaling molecules associated with P-gp reduction. Data from isolated brain capillaries from hAPP mice showed a reduction in P-gp protein expression levels relative to P-gp levels in WT mice, an effect that was blocked with PYR41 and PYR41/CSA treatment. Importantly, PYR41 and PYR41/CSA treatment did not alter protein expression levels of other proteins associated with A β production (hAPP), A β clearance (LRP1), A β transport (RAGE), or the degradation of P-gp (Nedd-4, 20S Proteasome).

Together, these data demonstrate that PYR41 treatment prevented P-gp ubiquitination in capillaries isolated from hAPP mice but did not affect other proteins involved in A β production or transport.

PYR41 Treatment of hAPP Mice Lowers A β Levels

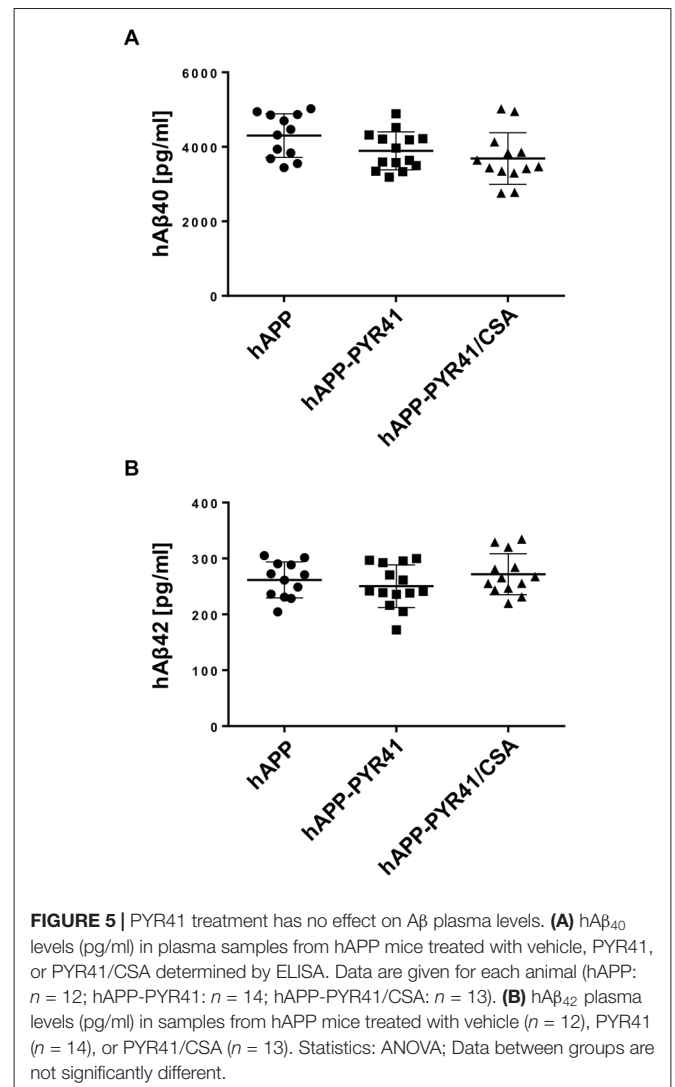
In a next step, we determined the consequences of PYR41 treatment on A β levels in plasma, capillary membranes, and brain tissue. We measured hA β ₄₀ and hA β ₄₂ levels in plasma by ELISA and found no difference in hA β ₄₀ and hA β ₄₂ plasma levels among PYR41-treated, PYR41/CSA-treated, and untreated hAPP mice (**Figures 5A,B**). Samples from WT mice were not included since WT mice do not express human A β .

We also immunostained isolated brain capillaries for hA β ₄₀ and hA β ₄₂ to determine capillary-associated A β levels. Brain capillaries isolated from vehicle-treated hAPP mice stained positive for both A β peptides (**Figures 6A,B**). PYR41-treatment decreased membrane-associated immunofluorescence of hA β ₄₀



by $16 \pm 5.2\%$ ($t = 8.9$, $p < 0.0001$; ANOVA *post hoc* test) and that of $hA\beta_{42}$ by $20 \pm 2.2\%$ ($t = 3.1$, $p = 0.0094$; ANOVA *post hoc* test) relative to untreated hAPP mice. However, this effect was not observed in $A\beta$ -immunostained brain capillaries from PYR41/CSA-treated hAPP mice, indicating that inhibiting P-gp transport activity with CSA blocks the reduction in $A\beta$ levels in brain capillaries.

Finally, data from Western blot analyses showed a significant reduction of $hA\beta_{40}$ and $hA\beta_{42}$ protein levels in brain tissue samples of PYR41-treated hAPP mice relative to untreated hAPP mice (Figure 7A). This was not the case in brain tissue from PYR41-treated mice that also received CSA to control for P-gp transport activity. Optical density measurements of Western blots revealed that PYR41 treatment reduced brain $hA\beta_{40}$ levels by $42 \pm 6.8\%$ ($t = 6.3$, $p < 0.003$; $df = 4$, t -test) and $hA\beta_{42}$ levels by $47 \pm 4.5\%$ ($t = 10.5$, $p < 0.0004$; $df = 4$, t -test) compared to vehicle-treated hAPP mice. Consistent with our Western blot



results, data from ELISA analysis of brain samples also showed a reduction in $hA\beta_{40}$ and $hA\beta_{42}$ brain levels in hAPP mice treated with PYR41. $hA\beta_{40}$ levels were reduced by $53.3 \pm 0.51\%$ ($t = 11.4$, $p = 0.0005$; ANOVA *post hoc* test) and $hA\beta_{42}$ levels were reduced by $33.3 \pm 0.08\%$ ($t = 4.9$, $p = 0.018$; ANOVA *post hoc* test), respectively (Figures 7B,C). Together these data indicate that PYR41 treatment prevents P-gp degradation, which results in a reduction in $hA\beta_{40}$ and $hA\beta_{42}$ brain levels in hAPP mice.

In summary, our data indicate that blocking P-gp ubiquitination prevents P-gp degradation, which ultimately leads to a reduction in $A\beta$ brain levels. Thus, targeting the ubiquitin-proteasome system early in AD could be a therapeutic strategy to protect brain capillary P-gp and thereby lower $A\beta$ brain levels.

DISCUSSION

We recently reported that P-gp protein expression and transport activity levels are significantly reduced at the blood-brain barrier

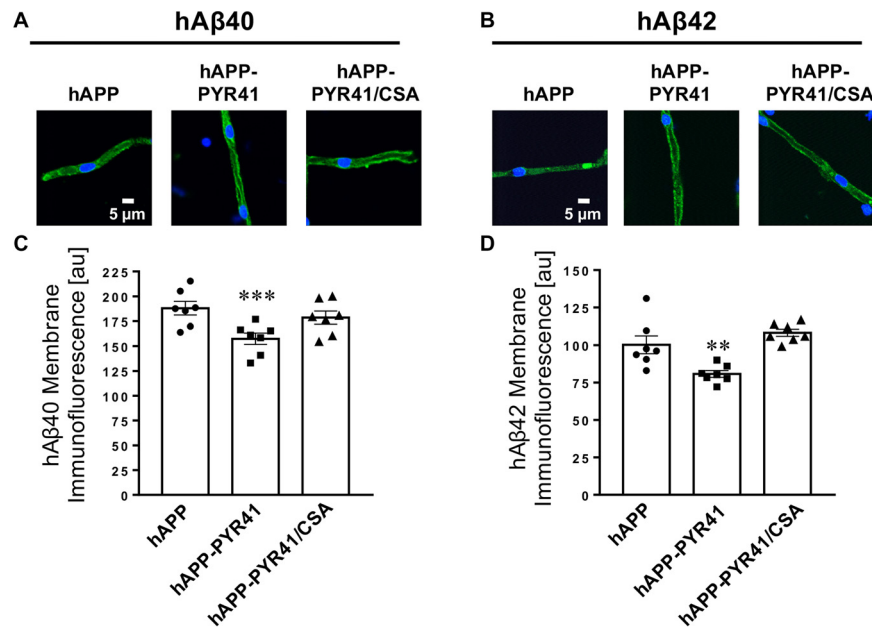


FIGURE 6 | PYR41 treatment reduces A β levels in brain capillary membranes. Representative confocal images of (A) hA β_{40} -immunostained and (B) hA β_{42} -immunostained brain capillaries isolated from vehicle-, PYR41- and PYR41/CSA-treated hAPP mice. Data from image analysis with ImageJ show that (C) hA β_{40} and (D) hA β_{42} membrane immunofluorescence is lower in capillaries isolated from PYR41-treated hAPP compared to control hAPP mice and mice that received PYR41/CSA. Data are mean \pm SEM ($n = 7$ brain capillaries per treatment group); shown are arbitrary fluorescence units (scale 0–255). Statistics: ** $p < 0.01$ (ANOVA), *** $p < 0.001$ (ANOVA) significantly lower than hAPP vehicle-treated mice.

in young, 12-week old hAPP mice that do not display cognitive deficits yet (Hartz et al., 2010). We also demonstrated that A β_{40} triggers reduction of P-gp expression and activity levels by activating the ubiquitin-proteasome system which leads to degradation of the transporter (Akkaya et al., 2015; Hartz et al., 2016). One consequence of reduced P-gp levels is impaired A β clearance from brain to blood across the blood-brain barrier (Hartz et al., 2010). The present study extends our previous *ex vivo* findings to an *in vivo* therapeutic strategy designed to prevent loss of P-gp by targeting the ubiquitin-proteasome system.

Here, we report that P-gp protein expression levels are reduced and P-gp ubiquitination levels are increased in isolated capillaries from AD patients relative to CNIs (Figure 1). Further, we show that treatment of 8–12-week old hAPP mice with PYR41, a specific and irreversible inhibitor of ubiquitin-activating enzyme E1, prevented degradation of P-gp in brain capillaries from hAPP mice (Figure 2). P-gp transport activity levels in PYR41-treated hAPP mice were comparable to those in control WT mice, and P-gp-mediated A β_{40} transport activity was also fully restored to control levels in brain capillaries isolated from PYR41-treated hAPP mice (Figure 3). We found that PYR41 treatment reduced levels of ubiquitinated P-gp in brain capillaries from hAPP mice, indicating successful inhibition of E1 function *in vivo* (Figure 4A). Other proteins involved in A β production and/or transport were not affected by PYR41 treatment (Figure 4B). While our data suggest that PYR41 treatment prevented P-gp ubiquitination in brain

capillaries isolated from hAPP mice without affecting proteins involved in A β production or transport (Figure 4B), we cannot fully exclude that PYR41 had no effect on other proteins that could also be involved in A β brain accumulation. PYR41 treatment did not affect A β plasma levels in hAPP mice, but slightly reduced hA β_{40} and hA β_{42} levels in brain capillaries (Figures 5, 6). PYR41 treatment did, however, significantly reduce hA β brain levels in PYR41-treated hAPP mice compared to vehicle- and PYR41/CSA-treated hAPP control mice (Figure 7).

Together, we provide *in vivo* evidence that inhibiting the ubiquitin-proteasome system blocks the reduction of P-gp levels and lowers A β brain levels in an AD mouse model. In the following sections we discuss different aspects of our study and put our findings in context with existing reports.

The Ubiquitin-Proteasome System Is Involved in P-gp Regulation

The ubiquitin-proteasome system is responsible for degradation of proteins, and therefore, essential for proteostasis (Ciechanover, 1994; Ciechanover and Kwon, 2015). The first step in protein degradation by the ubiquitin-proteasome system is ubiquitination of the target protein that is to be degraded. In a four-step process, a cascade of ubiquitin-activating, -conjugating, -ligating and -elongating enzymes (E1–E4) mediate the conjugation of ubiquitin to an amino group of the target protein. After addition of a polyubiquitin chain on the target protein, the now ubiquitinated membrane

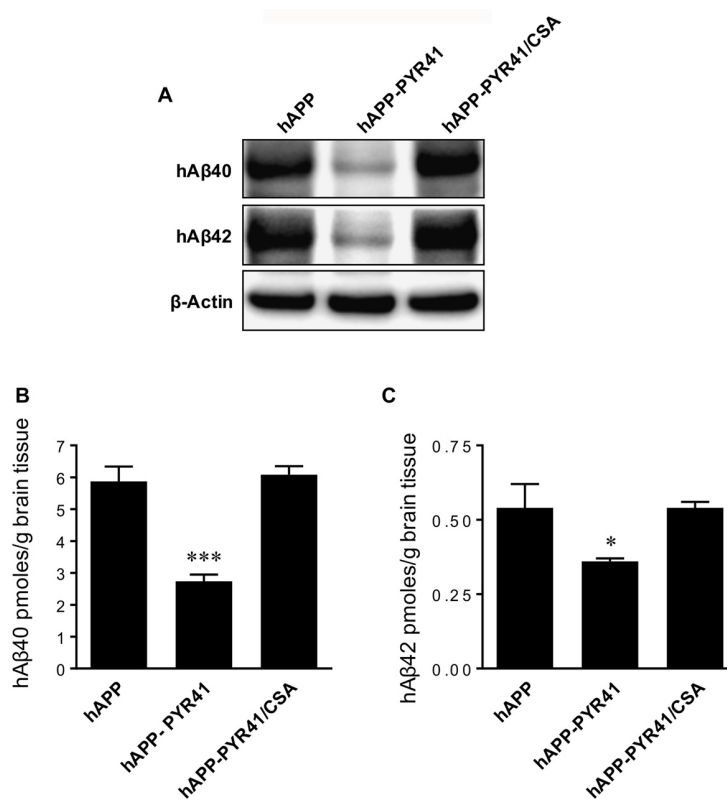


FIGURE 7 | PYR41 treatment reduces A β brain levels in hAPP mice. **(A)** Western blots showing PYR41 treatment reduced hA β_{40} and hA β_{42} protein expression levels in total brain tissue in hAPP mice compared to vehicle-treated WT mice or hAPP mice treated with PYR41/CSA; β -actin was used as protein loading control. ELISA analysis of brain tissue revealed that PYR41 significantly reduced protein levels of **(B)** hA β_{40} by $53.3 \pm 0.51\%$ and **(C)** hA β_{42} by $33.3 \pm 0.08\%$. Data are mean \pm SEM (pooled tissue from 15 mice per treatment group). Statistics: * $p < 0.05$ and *** $p < 0.001$ (ANOVA), significantly lower than hAPP vehicle-treated mice.

protein is internalized, recognized by the 26S proteasome complex and is then degraded in an ATP-driven process. The way proteins are ubiquitinated is complex and multifaceted. Some proteins are tagged with one ubiquitin molecule in a process referred to as monoubiquitination. Other proteins undergo multi-monoubiquitination during which different amino acid residues of the same target protein receive each one ubiquitin molecule. In contrast, polyubiquitination describes a process during which several ubiquitin molecules are added to one target protein resulting in linear or branched polyubiquitinated chains with different topologies. Mono- and polyubiquitination affects proteins in many ways: it can affect protein activity, promote or prevent protein interactions, alter protein cellular location or signal protein degradation via the proteasome.

Our previous work and the present study show that blood-brain barrier P-gp protein expression levels, and thus, P-gp transport activity levels, are regulated by the ubiquitin-proteasome system (Akkaya et al., 2015; Hartz et al., 2016). Our findings suggest that increased proteasomal degradation of P-gp is responsible for reduced P-gp expression and activity levels in AD. Our work is consistent with findings from other groups showing that the ubiquitin-proteasome system regulates localization, protein expression, and transport

function of human P-gp (Loo and Clarke, 1998; Zhang et al., 2004). Katayama et al. (2013) demonstrated in the human colorectal cancer cell lines HCT-15 and SW620 that FBXO15, a subunit of the ubiquitin E3 ligase, is a negative regulator of P-gp protein expression. Data from immunoprecipitation experiments indicated that FBXO15 binds to P-gp and enhances ubiquitination of the transporter. FBXO15 knockdown led to increased P-gp expression and transport activity in both cancer cell lines. In the same study, Katayama et al. (2013) also demonstrated that the ubiquitin E3 ligase complex SCFFbx15 recognizes P-gp as a substrate and brings the transporter in contact with the ubiquitin-conjugating enzyme Ube2r1, which ubiquitinates P-gp. More recently, Katayama et al. (2016) showed that inactivating MAPK signaling with small-molecule inhibitors leads to increased Ube2r1 expression levels, which, in turn, promotes P-gp degradation through the proteasome. Ravindranath et al. (2015) showed that the ubiquitin E3-ligase FBXO21 also catalyzes P-gp ubiquitination, thereby targeting it for subsequent proteasomal degradation. In addition, Rao et al. (2006) showed that the E3 ubiquitin ligase, RING finger protein 2 (RNF2), interacts with the linker region of human P-gp and the authors demonstrated that co-expression of RNF2 and P-gp results in decreased ATPase activity and proteolytic protection of the transporter in Sf9 insect cells. Together,

data from various groups suggest that P-gp expression and transport activity are regulated by the ubiquitin-proteasome system.

Our previously published work indicates that A β ₄₀ triggers P-gp ubiquitination, resulting in internalization and proteasomal degradation of the transporter (Hartz et al., 2016). Further, we have demonstrated that P-gp may be a substrate for the ubiquitin E3-ligase Nedd-4 (Akkaya et al., 2015). In the present study, we expand this line of research by inhibiting P-gp ubiquitination with the ubiquitin-activating enzyme E1 inhibitor PYR41 in a mouse AD model *in vivo* and show that blocking P-gp ubiquitination prevents loss of P-gp and lowers A β brain levels.

In addition to P-gp, other proteins are also thought to facilitate A β transport across the blood-brain barrier such as the low-density lipoprotein receptor-related protein (LRP; Deane et al., 2008; Storck et al., 2016). Similar to P-gp, LRP levels were reduced in brain capillaries from various AD mouse models and in post-mortem brain tissue from AD patients (Donahue et al., 2006; Silverberg et al., 2010). Like P-gp, degradation of LRP is mediated by the proteasome, however, LRP degradation appears to be independent from ubiquitination. In this regard, Melman et al. (2002) have demonstrated that tyrosine and di-leucine motifs within the LRP cytoplasmic tail mediate rapid endocytosis followed by proteasomal degradation, a process that does not require ubiquitination. Deane et al. (2004) showed that A β enhanced LRP proteasomal degradation in brain capillaries of 6–9-month old hAPP mice with cognitive impairment. The low LRP levels and the behavior deficits in these mice are consistent with reduced LRP levels in A β -accumulating mice and patients with AD and familial cerebrovascular β -amyloidosis (Deane et al., 2004). These findings suggest that reduced expression and activity levels of P-gp and LRP in brain capillaries, which contributes to A β pathology, result from similar augmentations of the ubiquitin-proteasome system, where P-gp is affected by enhanced ubiquitination and LRP is affected by enhanced direct proteasomal degradation.

The Ubiquitin-Proteasome System in Alzheimer's Disease

Protein misfolding, protein mishandling and deficits in protein quality control often drive neurodegenerative disease pathology (Urushitani et al., 2002; Kabashi et al., 2004; Ross and Pickart, 2004). These abnormal processes can lead to accumulation of A β in the brain and intraneuronal aggregation of hyper-phosphorylated tau protein, both of which are hallmarks of AD (Oddo, 2008; Riederer et al., 2011; Morawe et al., 2012; Hong et al., 2014; Gentier and van Leeuwen, 2015; Gadhave et al., 2016). Numerous studies reported that the activity of the ubiquitin-proteasome system is reduced in AD. For example, data from post-mortem studies of patients with late-stage AD showed accumulation of ubiquitin in both plaques and tangles and increased levels of a variety of ubiquitinated proteins (Perry et al., 1987; Keck et al., 2003). One explanation for this finding is a dysfunctional ubiquitin-proteasome system, where ubiquitinated proteins accumulate in the tissue but

are not further degraded by the proteasome. Indeed, Keller et al. (2000) observed a significant decrease in proteasome activity in the hippocampus, parahippocampal gyrus, middle temporal gyri, and inferior parietal lobule of patients with AD compared to cognitive normal individuals. Moreover, in AD, the proteolytic activity of the 26S proteasome appears to be impaired, resulting in oxidation and downregulation of ubiquitin C-terminal hydrolase 1 (UCH1), which is responsible for ubiquitin turnover (Almeida et al., 2006). Further, mutant ubiquitin, UBB⁺, is a hallmark of various neurodegenerative diseases. Elevated UBB⁺ levels in the brain directly inhibit proteasome activity, which is thought to lead to A β accumulation and hyper-phosphorylated tau, and thus, constitutes a risk factor for AD (Lindsten et al., 2002; van Leeuwen et al., 2006; Shabek et al., 2009; Dennissen et al., 2010; Ciechanover and Kwon, 2015). Collectively, growing evidence suggests that a dysfunctional ubiquitin-proteasome system contributes to AD pathology. However, little is known about the mechanisms that drive irregular activity of the complex ubiquitin-proteasome system, what brain regions and brain cell types are affected is not fully understood, and during which disease stages these changes occur is unclear. In contrast to brain tissue, our previous reports and the present study indicate that in the brain capillaries of the blood-brain barrier, the ubiquitin-proteasome system is overly active, leading to ubiquitination and degradation of membrane proteins such as P-gp (Akkaya et al., 2015; Hartz et al., 2016). The discrepancy between impaired proteasome activity in brain tissue and increased proteasome activity in brain capillary endothelial cells could be due to tissue-specific differences of the 20S proteasome. This explanation is supported by multiple reports showing that enzymes of the ubiquitin pathway (E1–4) are expressed in a tissue-specific manner and that alterations in ubiquitin ligase activity, proteasome subunit composition, and proteasome-interacting proteins are tissue-specific and adapt to functional needs in their respective tissues (Patel and Majetschak, 2007; Mayor and Peng, 2012; Kniepert and Groettrup, 2014; Ortega and Lucas, 2014).

In addition to tissue-specific differences, it is possible that proteasome activity changes with age, and thus, could be time- or even context-dependent. Current studies in our laboratory are aimed at determining levels of ubiquitination and 20S proteasome activity in hAPP mice at different ages.

The Ubiquitin-Proteasome System as a Therapeutic Target

Collectively, our previous and present findings suggest that the ubiquitin-proteasome system is involved in reducing P-gp protein expression and transport activity levels in AD. Based on data from our studies, preventing P-gp loss by targeting the ubiquitin-proteasome pathway could potentially serve as therapeutic strategy to protect P-gp from degradation, reduce A β brain accumulation, and slow AD progression. While targeting ubiquitination may represent a new therapeutic strategy, developing drugs that target the ubiquitin activating, conjugating, ligating and elongating enzymes E1–E4 remains a challenge. These enzymes do not have a well-defined catalytic

pocket, which makes the design of specific small molecule inhibitors difficult (Nalepa et al., 2006). Further, ubiquitination is a complex process that depends on dynamic protein-protein interactions that are difficult to disrupt with small molecules. In addition, as the name indicates, ubiquitination is a ubiquitous process present in all cells of the body, and thus, selectively targeting one tissue and not others is challenging. Consequently, FDA-approved drugs that specifically and selectively block ubiquitination are currently not available.

A different therapeutic option could be to target the proteasome itself. Currently, two FDA-approved small-molecule 20S proteasome inhibitors are on the market for cancer therapy: bortezomib (Velcade®) and carfilzomib (Krypolis®). Both drugs show efficacy in multiple myeloma with manageable pharmacokinetic properties and a relatively low side effect profile. Since the 20S proteasome subunit is the proteolytic core of the multi-subunit 26S proteasome proteolytic complex, both inhibitors—bortezomib and carfilzomib—also affect the activity of the entire 26S proteasome complex. While targeting the proteasome is an option, two points need more reflection. First, the potential inverse relationship between dysfunction of the ubiquitin-proteasome system in the brain relative to the blood-brain barrier must be taken into consideration. Inhibiting the 20S proteasome may be particularly beneficial in the early stages of AD to prevent P-gp loss and facilitate A β clearance. However, 20S proteasome inhibition may be detrimental in later AD stages when the ubiquitin-proteasome system is greatly impaired in the brain. Second, 20S proteasome inhibition is only feasible and can only be fully taken advantage of when AD is diagnosed early. While significant efforts have been made to identify biomarkers and develop novel imaging techniques that allow early AD diagnosis, no tools are currently available in the clinic and early AD diagnosis, prior to the appearance of behavioral symptoms, remains a formidable challenge.

In summary, in the present *in vivo* study we show that preventing ubiquitination of P-gp at the blood-brain barrier protects the transporter from degradation, which substantially lowers A β brain levels in an AD mouse model. These data suggest

REFERENCES

- Akkaya, B. G., Zolnerciks, J. K., Ritchie, T. K., Bauer, B., Hartz, A. M., Sullivan, J. A., et al. (2015). The multidrug resistance pump ABCB1 is a substrate for the ubiquitin ligase NEDD4-1. *Mol. Membr. Biol.* 32, 39–45. doi: 10.3109/09687688.2015.1023378
- Almeida, C. G., Takahashi, R. H., and Gouras, G. K. (2006). β -Amyloid accumulation impairs multivesicular body sorting by inhibiting the ubiquitin-proteasome system. *J. Neurosci.* 26, 4277–4288. doi: 10.1523/JNEUROSCI.5078-05.2006
- Carrano, A., Snkhchyan, H., Kooij, G., van der Pol, S., van Horsen, J., Veerhuis, R., et al. (2014). ATP-binding cassette transporters P-glycoprotein and breast cancer related protein are reduced in capillary cerebral amyloid angiopathy. *Neurobiol. Aging* 35, 565–575. doi: 10.1016/j.neurobiolaging.2013.09.015
- Chen, J.-Q., Wakefield, L. M., and Goldstein, D. J. (2015). Capillary nano-immunoassays: advancing quantitative proteomics analysis, biomarker assessment and molecular diagnostics. *J. Transl. Med.* 13:182. doi: 10.1186/s12967-015-0537-6
- Chiu, C., Miller, M. C., Monahan, R., Osgood, D. P., Stopa, E. G., and Silverberg, G. D. (2015). P-glycoprotein expression and amyloid accumulation

a novel therapeutic avenue that helps protect P-gp by limiting A β -induced P-gp degradation for improved A β clearance across the blood-brain barrier in AD.

AUTHOR CONTRIBUTIONS

AH and BB contributed to the major design, acquisition, analysis and interpretation of data for the work and wrote and revised the manuscript. YZ carried out ELISAs and experiments with isolated human capillaries. AS contributed to Western blot data analysis and drafted parts of the manuscript. EA provided all statistical analyses. All authors were involved in drafting and revising the work for important intellectual content. All authors approved the final version and agreed to be accountable for all aspects of the work in ensuring that questions related to the accuracy or integrity of any part of the work are appropriately investigated and resolved.

FUNDING

This project was supported by Grant No. 2R01AG039621 from the National Institute on Aging (to AH). The content is solely the responsibility of the authors and does not necessarily represent the official views of the National Institute on Aging or the National Institutes of Health.

ACKNOWLEDGMENTS

We thank the members of the Hartz and Bauer laboratories for proofreading the manuscript.

SUPPLEMENTARY MATERIAL

The Supplementary Material for this article can be found online at: <https://www.frontiersin.org/articles/10.3389/fnagi.2018.00186/full#supplementary-material>

- in human aging and Alzheimer's disease: preliminary observations. *Neurobiol. Aging* 36, 2475–2482. doi: 10.1016/j.neurobiolaging.2015.05.020
- Ciechanover, A. (1994). The ubiquitin-proteasome proteolytic pathway. *Cell* 79, 13–21. doi: 10.1016/0092-8674(94)90396-4
- Ciechanover, A., and Kwon, Y. T. (2015). Degradation of misfolded proteins in neurodegenerative diseases: therapeutic targets and strategies. *Exp. Mol. Med.* 47:e147. doi: 10.1038/emmm.2014.117
- Cirrito, J. R., Deane, R., Fagan, A. M., Spinner, M. L., Parsadanian, M., Finn, M. B., et al. (2005). P-glycoprotein deficiency at the blood-brain barrier increases amyloid- β deposition in an Alzheimer disease mouse model. *J. Clin. Invest.* 115, 3285–3290. doi: 10.1172/JCI25247
- Deane, R., Sagare, A., Hamm, K., Parisi, M., Lane, S., Finn, M. B., et al. (2008). apoE isoform-specific disruption of amyloid β peptide clearance from mouse brain. *J. Clin. Invest.* 118, 4002–4013. doi: 10.1172/JCI36663
- Deane, R., Wu, Z., Sagare, A., Davis, J., Du Yan, S., Hamm, K., et al. (2004). LRP/amyloid β -peptide interaction mediates differential brain efflux of A β isoforms. *Neuron* 43, 333–344. doi: 10.1016/j.neuron.2004.07.017
- Dennissen, F., Kholod, N., Steinbusch, H., and Van Leeuwen, F. (2010). Misframed proteins and neurodegeneration: a novel view on Alzheimer's and Parkinson's diseases. *Neurodegener. Dis.* 7, 76–79. doi: 10.1159/000285510

- Deo, A. K., Borson, S., Link, J. M., Domino, K., Eary, J. F., Ke, B., et al. (2014). Activity of P-glycoprotein, a β -amyloid transporter at the blood-brain barrier, is compromised in patients with mild Alzheimer disease. *J. Nucl. Med.* 55, 1106–1111. doi: 10.2967/jnumed.113.130161
- Donahue, J. E., Flaherty, S. L., Johanson, C. E., Duncan, J. A., Silverberg, G. D., Miller, M. C., et al. (2006). RAGE, LRP-1 and amyloid- β protein in Alzheimer's disease. *Acta Neuropathol.* 112, 405–415. doi: 10.1007/s00401-006-0115-3
- Gadhav, K., Bolshette, N., Ahire, A., Pardeshi, R., Thakur, K., Trandafir, C., et al. (2016). The ubiquitin proteasomal system: a potential target for the management of Alzheimer's disease. *J. Cell. Mol. Med.* 20, 1392–1407. doi: 10.1111/jcmm.12817
- Gentier, R. J., and van Leeuwen, F. W. (2015). Misframed ubiquitin and impaired protein quality control: an early event in Alzheimer's disease. *Front. Mol. Neurosci.* 8:47. doi: 10.3389/fnmol.2015.00047
- Guan, H., and Ricciardi, R. P. (2012). Transformation by E1A oncoprotein involves ubiquitin-mediated proteolysis of the neuronal and tumor repressor REST in the nucleus. *J. Virol.* 86, 5594–5602. doi: 10.1128/JVI.06811-11
- Hardy, J., and Selkoe, D. J. (2002). The amyloid hypothesis of Alzheimer's disease: progress and problems on the road to therapeutics. *Science* 297, 353–356. doi: 10.1126/science.1072994
- Hartz, A. M., Bauer, B., Block, M. L., Hong, J. S., and Miller, D. S. (2008). Diesel exhaust particles induce oxidative stress, proinflammatory signaling and P-glycoprotein up-regulation at the blood-brain barrier. *FASEB J.* 22, 2723–2733. doi: 10.1096/fj.08-106997
- Hartz, A. M., Bauer, B., Fricker, G., and Miller, D. S. (2004). Rapid regulation of P-glycoprotein at the blood-brain barrier by endothelin-1. *Mol. Pharmacol.* 66, 387–394. doi: 10.1124/mol.104.001503
- Hartz, A. M., Bauer, B., Soldner, E. L., Wolf, A., Boy, S., Backhaus, R., et al. (2012). Amyloid- β contributes to blood-brain barrier leakage in transgenic human amyloid precursor protein mice and in humans with cerebral amyloid angiopathy. *Stroke* 43, 514–523. doi: 10.1161/STROKEAHA.111.627562
- Hartz, A. M., Miller, D. S., and Bauer, B. (2010). Restoring blood-brain barrier P-glycoprotein reduces brain amyloid- β in a mouse model of Alzheimer's disease. *Mol. Pharmacol.* 77, 715–723. doi: 10.1124/mol.109.061754
- Hartz, A. M., Pekcec, A., Soldner, E. L., Zhong, Y., Schlichtiger, J., and Bauer, B. (2017). P-gp protein expression and transport activity in rodent seizure models and human epilepsy. *Mol. Pharm.* 14, 999–1011. doi: 10.1021/acs.molpharmaceut.6b00770
- Hartz, A. M., Zhong, Y., Wolf, A., LeVine, H., III, Miller, D. S., and Bauer, B. (2016). A β 40 reduces P-glycoprotein at the blood-brain barrier through the ubiquitin-proteasome pathway. *J. Neurosci.* 36, 1930–1941. doi: 10.1523/JNEUROSCI.0350-15.2016
- Hong, L., Huang, H.-C., and Jiang, Z.-F. (2014). Relationship between amyloid- β and the ubiquitin-proteasome system in Alzheimer's disease. *Neurol. Res.* 36, 276–282. doi: 10.1179/1743132813Y.0000000288
- Jeynes, B., and Provias, J. (2011). The case for blood-brain barrier dysfunction in the pathogenesis of Alzheimer's disease. *J. Neurosci. Res.* 89, 22–28. doi: 10.1002/jnr.22527
- Kabashi, E., Agar, J. N., Taylor, D. M., Minotti, S., and Durham, H. D. (2004). Focal dysfunction of the proteasome: a pathogenic factor in a mouse model of amyotrophic lateral sclerosis. *J. Neurochem.* 89, 1325–1335. doi: 10.1111/j.1471-4159.2004.02453.x
- Katayama, K., Fujiwara, C., Noguchi, K., and Sugimoto, Y. (2016). RSK1 protects P-glycoprotein/ABCB1 against ubiquitin-proteasomal degradation by downregulating the ubiquitin-conjugating enzyme E2 R1. *Sci. Rep.* 6:36134. doi: 10.1038/srep36134
- Katayama, K., Noguchi, K., and Sugimoto, Y. (2013). FBXO15 regulates P-glycoprotein/ABCB1 expression through the ubiquitin-proteasome pathway in cancer cells. *Cancer Sci.* 104, 694–702. doi: 10.1111/cas.12145
- Keck, S., Nitsch, R., Grune, T., and Ullrich, O. (2003). Proteasome inhibition by paired helical filament-tau in brains of patients with Alzheimer's disease. *J. Neurochem.* 85, 115–122. doi: 10.1046/j.1471-4159.2003.01642.x
- Keller, J. N., Hanni, K. B., and Markesbery, W. R. (2000). Impaired proteasome function in Alzheimer's disease. *J. Neurochem.* 75, 436–439. doi: 10.1046/j.1471-4159.2000.0750436.x
- Kniepert, A., and Groettrup, M. (2014). The unique functions of tissue-specific proteasomes. *Trends Biochem. Sci.* 39, 17–24. doi: 10.1016/j.tibs.2013.10.004
- Kuhnke, D., Jedlitschky, G., Grube, M., Krohn, M., Jucker, M., Mosyagin, I., et al. (2007). MDR1-P-glycoprotein (ABCB1) mediates transport of Alzheimer's amyloid- β peptides—implications for the mechanisms of A β clearance at the blood-brain barrier. *Brain Pathol.* 17, 347–353. doi: 10.1111/j.1750-3639.2007.00075.x
- Lam, F. C., Liu, R. H., Lu, P. H., Shapiro, A. B., Renoir, J. M., Sharom, F. J., et al. (2001). β -Amyloid efflux mediated by p-glycoprotein. *J. Neurochem.* 76, 1121–1128. doi: 10.1046/j.1471-4159.2001.00113.x
- Lindsten, K., de Vrij, F. M., Verhoef, L. G., Fischer, D. F., van Leeuwen, F. W., Hol, E. M., et al. (2002). Mutant ubiquitin found in neurodegenerative disorders is a ubiquitin fusion degradation substrate that blocks proteasomal degradation. *J. Cell Biol.* 157, 417–427. doi: 10.1083/jcb.200111034
- Loo, T. W., and Clarke, D. M. (1998). Quality control by proteases in the endoplasmic reticulum removal of a protease-sensitive site enhances expression of human P-glycoprotein. *J. Biol. Chem.* 273, 32373–32376. doi: 10.1074/jbc.273.49.32373
- Mawuenyega, K. G., Sigurdson, W., Ovod, V., Munsell, L., Kasten, T., Morris, J. C., et al. (2010). Decreased clearance of CNS β -amyloid in Alzheimer's disease. *Science* 330, 1774–1774. doi: 10.1126/science.1197623
- Mayor, U., and Peng, J. (2012). Deciphering tissue-specific ubiquitylation by mass spectrometry. *Methods Mol. Biol.* 832, 65–80. doi: 10.1007/978-1-61779-474-2_3
- Mehta, D. C., Short, J. L., and Nicolazzo, J. A. (2013). Altered brain uptake of therapeutics in a triple transgenic mouse model of Alzheimer's disease. *Pharm. Res.* 30, 2868–2879. doi: 10.1007/s11095-013-1116-2
- Melman, L., Geuze, H. J., Li, Y., McCormick, L. M., Van Kerkhof, P., Strous, G. J., et al. (2002). Proteasome regulates the delivery of LDL receptor-related protein into the degradation pathway. *Mol. Biol. Cell* 13, 3325–3335. doi: 10.1091/mbc.e02-03-0152
- Mirra, S. S., Heyman, A., McKeel, D., Sumi, S., Crain, B. J., Brownlee, L., et al. (1991). The consortium to establish a registry for Alzheimer's disease (CERAD) part II. Standardization of the neuropathologic assessment of Alzheimer's disease. *Neurology* 41:479. doi: 10.1212/wnl.41.4.479
- Morawe, T., Hiebel, C., Kern, A., and Behl, C. (2012). Protein homeostasis, aging and Alzheimer's disease. *Mol. Neurobiol.* 46, 41–54. doi: 10.1007/s12035-012-8246-0
- Nalepa, G., Rolfe, M., and Harper, J. W. (2006). Drug discovery in the ubiquitin-proteasome system. *Nat. Rev. Drug Discov.* 5, 596–613. doi: 10.1038/nrd2056
- Nelson, P. T., Jicha, G. A., Schmitt, F. A., Liu, H., Davis, D. G., Mendiondo, M. S., et al. (2007). Clinicopathologic correlations in a large Alzheimer disease center autopsy cohort: neuritic plaques and neurofibrillary tangles “do count” when staging disease severity. *J. Neuropathol. Exp. Neurol.* 66, 1136–1146. doi: 10.1097/nen.0b013e31815c5efb
- Oddo, S. (2008). The ubiquitin-proteasome system in Alzheimer's disease. *J. Cell. Mol. Med.* 12, 363–373. doi: 10.1111/j.1582-4934.2008.00276.x
- O'Neill, R. A., Bhamidipati, A., Bi, X., Deb-Basu, D., Cahill, L., Ferrante, J., et al. (2006). Isoelectric focusing technology quantifies protein signaling in 25 cells. *Proc. Natl. Acad. Sci. U S A* 103, 16153–16158. doi: 10.1073/pnas.0607973103
- Ortega, Z., and Lucas, J. J. (2014). Ubiquitin-proteasome system involvement in Huntington's disease. *Front. Mol. Neurosci.* 7:77. doi: 10.3389/fnmol.2014.00077
- Park, R., Kook, S., Park, J., and Mook-Jung, I. (2014). A β 1–42 reduces P-glycoprotein in the blood-brain barrier through RAGE-NF- κ B signaling. *Cell Death Dis.* 5:e1299. doi: 10.1038/cddis.2014.258
- Patel, M. B., and Majetschak, M. (2007). Distribution and interrelationship of ubiquitin proteasome pathway component activities and ubiquitin pools in various porcine tissues. *Physiol. Res.* 56, 341–350.
- Perry, G., Friedman, R., Shaw, G., and Chau, V. (1987). Ubiquitin is detected in neurofibrillary tangles and senile plaque neurites of Alzheimer disease brains. *Proc. Natl. Acad. Sci. U S A* 84, 3033–3036. doi: 10.1073/pnas.84.9.3033
- Rao, P. S., Mallya, K. B., Srivenugopal, K. S., Balaji, K., and Rao, U. S. (2006). RNF2 interacts with the linker region of the human P-glycoprotein. *Int. J. Oncol.* 29, 1413–1419.
- Ravindranath, A. K., Kaur, S., Wernyj, R. P., Kumaran, M. N., Miletti-Gonzalez, K. E., Chan, R., et al. (2015). CD44 promotes multi-drug resistance by protecting P-glycoprotein from FBXO21-mediated ubiquitination. *Oncotarget* 6, 26308–26321. doi: 10.18632/oncotarget.4763

- Riederer, B. M., Leuba, G., Vernay, A., and Riederer, I. M. (2011). The role of the ubiquitin proteasome system in Alzheimer's disease. *Exp. Biol. Med.* 236, 268–276. doi: 10.1258/ebm.2010.010327
- Ross, C. A., and Pickart, C. M. (2004). The ubiquitin-proteasome pathway in Parkinson's disease and other neurodegenerative diseases. *Trends Cell Biol.* 14, 703–711. doi: 10.1016/j.tcb.2004.10.006
- Shabek, N., Herman-Bachinsky, Y., and Ciechanover, A. (2009). Ubiquitin degradation with its substrate, or as a monomer in a ubiquitination-independent mode, provides clues to proteasome regulation. *Proc. Natl. Acad. Sci. U S A* 106, 11907–11912. doi: 10.1073/pnas.0905746106
- Silverberg, G. D., Messier, A. A., Miller, M. C., Machan, J. T., Majmudar, S. S., Stopa, E. G., et al. (2010). Amyloid efflux transporter expression at the blood-brain barrier declines in normal aging. *J. Neuropathol. Exp. Neurol.* 69, 1034–1043. doi: 10.1097/NEN.0b013e3181f46e25
- Storck, S. E., Meister, S., Nahrath, J., Meißner, J. N., Schubert, N., Di Spiezio, A., et al. (2016). Endothelial LRP1 transports amyloid- β_{1-42} across the blood-brain barrier. *J. Clin. Invest.* 126, 123–136. doi: 10.1172/JCI81108
- Urushitani, M., Kurisu, J., Tsukita, K., and Takahashi, R. (2002). Proteasomal inhibition by misfolded mutant superoxide dismutase 1 induces selective motor neuron death in familial amyotrophic lateral sclerosis. *J. Neurochem.* 83, 1030–1042. doi: 10.1046/j.1471-4159.2002.01211.x
- van Assema, D. M., Lubberink, M., Bauer, M., van der Flier, W. M., Schuit, R. C., Windhorst, A. D., et al. (2012). Blood-brain barrier P-glycoprotein function in Alzheimer's disease. *Brain* 135, 181–189. doi: 10.1093/brain/awr298
- van Leeuwen, F., van Tijn, P., Sonnemans, M., Hobo, B., Mann, D., Van Broeckhoven, C., et al. (2006). Frameshift proteins in autosomal dominant forms of Alzheimer disease and other tauopathies. *Neurology* 66, S86–S92. doi: 10.1212/01.wnl.0000193882.46003.6d
- Wang, W., Bodles-Brakhop, A. M., and Barger, S. W. (2016). A role for P-glycoprotein in clearance of alzheimer amyloid β -peptide from the brain. *Curr. Alzheimer Res.* 13, 615–620. doi: 10.2174/1567205013666160314151012
- Wenger, R. M. (1986). Cyclosporine and analogues— isolation and synthesis— mechanism of action and structural requirements for pharmacological activity. *Fortschr. Chem. Org. Naturst.* 50, 123–168. doi: 10.1007/978-3-7091-8888-0_4
- Wijesuriya, H. C., Bullock, J. Y., Faull, R. L., Hladky, S. B., and Barrand, M. A. (2010). ABC efflux transporters in brain vasculature of Alzheimer's subjects. *Brain Res.* 1358, 228–238. doi: 10.1016/j.brainres.2010.08.034
- Yang, Y., Kitagaki, J., Dai, R.-M., Tsai, Y. C., Lorick, K. L., Ludwig, R. L., et al. (2007). Inhibitors of ubiquitin-activating enzyme (E1), a new class of potential cancer therapeutics. *Cancer Res.* 67, 9472–9481. doi: 10.1158/0008-5472.CAN-07-0568
- Yuede, C. M., Lee, H., Restivo, J. L., Davis, T. A., Hettinger, J. C., Wallace, C. E., et al. (2016). Rapid *in vivo* measurement of β -amyloid reveals biphasic clearance kinetics in an Alzheimer's mouse model. *J. Exp. Med.* 213, 677–685. doi: 10.1084/jem.20151428
- Zhang, Z., Wu, J.-Y., Hait, W. N., and Yang, J.-M. (2004). Regulation of the stability of P-glycoprotein by ubiquitination. *Mol. Pharmacol.* 66, 395–403. doi: 10.1124/mol.104.001966
- Zlokovic, B. V. (2005). Neurovascular mechanisms of Alzheimer's neurodegeneration. *Trends Neurosci.* 28, 202–208. doi: 10.1016/j.tins.2005.02.001

Conflict of Interest Statement: The authors declare that the research was conducted in the absence of any commercial or financial relationships that could be construed as a potential conflict of interest.

Copyright © 2018 Hartz, Zhong, Shen, Abner and Bauer. This is an open-access article distributed under the terms of the Creative Commons Attribution License (CC BY). The use, distribution or reproduction in other forums is permitted, provided the original author(s) and the copyright owner are credited and that the original publication in this journal is cited, in accordance with accepted academic practice. No use, distribution or reproduction is permitted which does not comply with these terms.